



Validation of thermal simulations of a non-air-conditioned office building in different seasonal, occupancy and ventilation conditions



I. Calixto-Aguirre, G. Huelsz*, G. Barrios, M.V. Cruz-Salas

Instituto de Energías Renovables, Universidad Nacional Autónoma de México, A.P. 34, 62580, Temixco, Morelos, Mexico

ARTICLE INFO

Keywords:
Building thermal simulation
Non-air-conditioned
Validation
Calibration
EnergyPlus
Experimental data

ABSTRACT

In this work, a methodology for the validation of non-air-conditioned building thermal simulations is proposed. Having certainty in these simulations can give confidence to building designers on the possibility to avoid the use of mechanical air-conditioned systems or to reduce the period of their use, thus increasing the building's energy efficiency. The main features of the proposed methodology that differentiate it from the previous ones are: i) the separation of data inputs which values are known with uncertainty into those that have more influence on indoor air temperature and those with more impact on surface temperatures; ii) to carry out the calibration process in two stages having as comparison variables indoor air temperature in the first stage and adding surface temperatures in the second stage; and iii) to carry out the validation process in different seasonal, occupancy and ventilation conditions. The case study is an office building, simulations are performed in EnergyPlus employing the Airflow Network model for infiltration and ventilation. Quantitative comparisons are made using eight metrics. The results show the advantages of carrying out the second stage of validation proposed in this work. The validation results show that the building model obtained from the calibration process is suitable to simulate the building in different seasonal, occupancy and ventilation conditions, and can be used with certainty to test strategies to improve thermal comfort in the building. For the case study, two strategies are tested showing important reductions in thermal discomfort on occupancy hours during the critical hot season.

1. Introduction

About 30% of total worldwide energy consumption and carbon emissions into the atmosphere correspond to the building sector [1]. Thus, it is of great importance to reduce the energy consumed by buildings.

1.1. Building's thermal and energy modeling and simulation

The modeling and simulation of building's thermal and energy performance is an important element in the design of energy efficient buildings. Three reviews of building modeling and energy performance prediction were recently published [2–4]. In Ref. [2], the modeling types are classified into physical models, statistical methods and hybrid models. The physical models are divided in turn into computational fluid mechanics (CFD) approach, zonal approach and multizone or nodal approach; the fundamentals, advantages, application area and limitations for each one were presented in the review. In Ref. [3], the classification is similar but employs different names: forward approach, data

driven approach and gray box approach. In Ref. [4], the focus is on the zonal modeling for large space buildings. In the multizone or nodal approach each building zone is considered a homogeneous volume characterized by uniform state variables and is approximated to a node, which generally represents a room [2]. This approach is useful to simulate buildings with many rooms. It is used to identify new strategies to improve energy efficiency in new or existing buildings. EnergyPlus is one of the most popular softwares using the nodal approach and is likewise an open source software. It is comprised by a collection of many program modules that take into account weather, thermal and mass loads in spaces, heat transfer through walls, roofs, floors and windows and also accounts for heat and mass transfer into buildings due to infiltration and ventilation [5].

1.2. Validation of thermal and energy building simulations

The validation of thermal and energy building simulations of existing buildings with their corresponding experimental measurements are undertaken so as to have reliable identification of energy savings or thermal comfort measures in an existing building and also to improve

* Corresponding author.

E-mail address: ghl@ier.unam.mx (G. Huelsz).

Available online 29 June 2021

<https://doi.org/10.1016/j.jobe.2021.102981> rights reserved.

Received 5 February 2021; Received in revised form 16 June 2021; Accepted 21 June 2021

Nomenclature	
AE	Absolute error [%]
ACH	Air changes per hour [1/h]
<i>b</i>	Intercept [°C]
CVRMSE	Coefficient of variation of the root mean square error [%]
DE	Defect error [%]
Δdf	Difference between simulated and experimental decrement factor [-]
Δlg	Difference between simulated and experimental lag time [h]
ΔT_{max}	Average of the difference between simulated and experimental daily maximum temperature [°C]
ΔT_{mean}	Average of the difference between simulated and experimental daily mean temperature [°C]
ΔT_{min}	Average of the difference between simulated and experimental daily minimum temperature [°C]
EE	Excess error [%]
GOF	Goodness of fit [-]
<i>m</i>	Slope [-]
MBE	Mean bias error [°C]
ME	Mean error [%]
NMBE	Normalized mean bias error [%]
<i>r</i>	Pearson's index [-]
RMSE	Root mean square error [°C]
<i>R</i> 2	Correlation coefficient [-]
<i>T_i</i>	Indoor air temperature [°C]
\bar{T}_i	Time average of <i>T_i</i> [°C]
<i>T_{si}</i>	Inside surface temperature [°C]
<i>T_{sis}</i>	Inside surface temperature of the South wall [°C]
<i>T_{siw}</i>	Inside surface temperature of the West wall [°C]
<i>T_{sir}</i>	Inside surface temperature of the roof wall [°C]
<i>T_{so}</i>	Outside surface temperature [°C]
<i>T_{sos}</i>	Outside surface temperature of the South wall [°C]
TE	Total error [%]
<i>exp</i>	Subindex indicating quantity from experiments
<i>sim</i>	Subindex indicating quantity from simulations
Acronyms	
AFN	Airflow Network model
ePMV	Extended Predicted Mean Value
NO	Unoccupied
O	Occupied

simulation skills of personnel with the aim of increasing the confidence in building simulations during the design stage of new buildings.

A literature review on calibration of building energy simulation programs was published in 2005 [6]. In this review, the uses, problems, procedures, uncertainty and tools of the calibration of building energy simulation programs were addressed, only air-conditioned building were considered. Most of the studies analyzed model errors using monthly data. Particular attention was paid to the calibration of the program DOE-2, which is the precursor of EnergyPlus. Raftery et al. [7] reported a review of case studies and methods for calibrating building energy models with measured data. They proposed an evidence-based methodology for the calibration of air-conditioned buildings using hourly data. Pernetti et al. [8] gave guidelines for the calibration of building simulations with the aim to reduce the discrepancies between simulated and actual building energy behavior. In these guidelines, the validation process consists of the calibration of the building model divided into five steps, and the validation over a different time period. The five steps are: 1) definition of the aim and the validation criteria; 2) general data gathering and base model definition; 3) sensitivity analysis; 4) second data gathering campaign and simulations runs; and 5) calibration criteria. Detailed information is given concerning the five steps of calibration using either one of two study cases, a non-air-conditioned historical building that was unoccupied and without internal heat gains, and an occupied air-conditioned house. In the case of the non-air-conditioned building, one space was instrumented with air temperature and surface temperature sensors and was used as the control thermal zone. Comparisons between simulated and measured temperatures were made qualitatively and quantitatively, the latter employing three metrics. Results for the final building model are within the following ranges for both the indoor air and the surface temperatures: 0.5–1.0 °C for the mean bias error (MBE), 0.9–1.0 °C for the root mean square error (RMSE) and 0.99 to 1.00 for Pearson's index (*r*). The simulations were made using TRNSYS.

1.3. Comparison of EnergyPlus results with experimental results

EnergyPlus is being constantly used by both professionals and researchers. Nearly 2000 scientific articles can be found that report the use of this program. However, there are only eight articles that report on the comparison of EnergyPlus simulated results with experimental results,

most of which are focused on a specific problem and do not report the validation process. All of these articles include a description of the studied building, information of the measured weather variables as well as the variables used for the comparison between simulations and measurements. A brief description of the building and the main results of the comparison between simulations and measurements are presented for each case.

Sang et al. [9] studied a full-scale non-air-conditioned test room which included a wall with a phase change material. The comparison variables were *T_i* and *T_{si}*. A qualitative comparison of *T_{si}* for the four walls was made by plotting each during one full day.

Raftery et al. [10] studied the effect of vertical greenery systems (VGS) on the building's thermal performance. The comparison variables were *T_i*, *T_{so}* and *T_{si}*. The cases of study were: A) a test cell with a VGS on the west wall and B) two residential flats on a thirty-three story building, one with VGS and the second without VGS. *R*2, the cosine and the norm were used as metrics for the comparison between simulations and measurements. The norm is zero and the cosine is one for a perfect agreement. The metric results for *T_i* are: *R*2 equals 0.97 and 0.81, in the case A) and B), respectively. The norm was between 0.02 and 0.09 and the cosine from 0.60 to 0.95, for both cases.

Andelković et al. [11] modeled a double skin façade (DSF) of a five story air-conditioned building. The variables compared were: indoor air temperature (*T_i*), inside surface temperature (*T_{si}*), outside surface temperature (*T_{so}*), and air velocity in the DSF. The metric results for *T_i* were: *R*2 = 0.93, MBE = -2.25 °C, RMSE = 2.58 °C, the coefficient of variation of the root mean square error CVRMSE = 12.29%, ΔT_{max} = 5.54 °C and ΔT_{min} = 0.01 °C.

Simá et al. [12] studied the shading effect of both a tree and neighboring buildings on the thermal performance of a closed and unoccupied house. Simulations on the shading effect with and without the tree were carried out and validated with the experimental measurements. The variables of comparison were *T_i*, *T_{si}* and *T_{so}* of one thermal zone. The metrics were the differences of decrement factor (Δdf), lag time (Δlg) and discomfort hours.

Yang et al. [13] evaluated three different heat balance algorithms: conduction transfer functions, combined heat and moisture transfer model and effective moisture penetration depth. A full-scale air-conditioned test room with 2 occupants was used. Three different climates were simulated: hot humid, temperate and hot dry. *T_i* simulated



(2021) 102922

Fig. 1. Views of the building. Aerial view, view of the South façade and view of the North façade.

and T_i measured were qualitatively compared by plotting them.

Barrios et al. [14] validated the equivalent-homogeneous-layers-set method (EHLS) implemented into EnergyPlus. The validation was made for a full-scale test room. Maximum differences are $\Delta T_{max} = -0.9^\circ\text{C}$, $\Delta f = 0.1$ and $\Delta g = 1.9$ h.

Barbaresi et al. [15] studied an air-conditioned wine storage building. Two models were simulated: A) considering a single thermal zone and B) considering two thermal zones. The comparison variable was T_i and the metrics were r, slope (m), and intercept (b) of the linear regression, mean error (ME), RMSE, total error (TE), excess error (EE), defect error (DE), and absolute error (AE). The results for model A were: $r = 0.994$, $m = 1.013$, $b = -0.5^\circ\text{C}$ and RMSE = 0.705°C . The results for model B were: $r = 0.994$, $m = 0.994$, $b = -0.1^\circ\text{C}$ and RMSE = 0.684°C . As expected the results obtained in the simulation with two thermal zones were more accurate.

Belleri et al. [16] described an analysis of the predicted and measured ventilation performance of an non-air-conditioned office in California, using the air changes per hour (ACH) as a comparison variable. At first the office was modeled as if it had not yet been constructed, considering values for some input variables derived from the literature. Wind-pressure coefficients were measured in wind-tunnel experiments. Measurements of T_i , and the window opening factors of the windows and doors were conducted in the office. The model was incrementally improved by changing the following parameters: alignment of T_i to the measured value by adjusting the heating and cooling set-points of an EnergyPlus ideal air-conditioning system; window control from the ASHRAE-55-Adaptive to the Temperature method; weather data frequency from 1 h to 5 min; window control as measured; and wind-pressure coefficients from measurements. The authors pointed out that the process highlighted the limitations of the occupant-driven window control models of EnergyPlus.

Raftery et al. [17] described the calibration process of an air-conditioned office building using the method proposed in Ref. [7]. The metrics for the comparison were the MBE and CVRMSE for the HVAC electric consumption. The results for the final model were: MBE

= 4.1% and CVRMSE = 7.8%.

Coakley et al. [18] described the simulation calibration process of a library building with mixed-mode ventilation. The input data was divided into different classes each with a different range of variation (0–50%) as related to the certainty of the data. One hundred simulations with random input data were performed. The metrics for the comparison were the normalized mean bias error (NMBE), CVRMSE and goodness of fit (GOF), for electric energy consumption and for T_i . They compared metrics derived from monthly and hourly data, pointing out that monthly data masks model discrepancies.

1.4. Simulations for non-air conditioned office buildings

In Mexico there are regions of the country where designing buildings with a bioclimatic approach, which includes the use of natural ventilation, can provide thermal comfort to its occupants without the use of air-conditioning systems. Nevertheless, the use of air-conditioning is increasing specially the case of office buildings. Accurate thermal building simulations of non-air-conditioned buildings can give confidence to building designers on the possibility to avoid the use of mechanical air-conditioned systems or to likewise help reduce their time of usage, increasing the building's overall energy efficiency.

EnergyPlus simulations have been used to study the thermal performance of non-air-conditioned office buildings. Some examples of these studies are: the evaluation of different ventilation strategies for space cooling, where EnergyPlus simulations were complemented with computational fluid dynamics (CFD) simulations [19]; the impact of climate change on thermal comfort [20]; the impact of outdoor airborne particulate matter with an aerodynamic diameter below $2.5\text{ }\mu\text{m}$ (PM2.5) on natural ventilation usability in California [21]; and the suitability of phase change materials coupled with night ventilation in Western China [22].

Table 1
Equipment and uncertainty for each weather variable.

Variable	Equipment	Uncertainty
Beam radiation	Pyrheliometer EKO MS-56/ISO 9060 first class	<1W/m ²
Diffuse radiation	Pyranometer Kipp & Zonen CMP11/Iso 9060 class A	<10W/m ²
Wind speed	Wind sonic anemometer Gill instrument option 4	±2% (at 12 m/s)
Wind direction	Wind sonic anemometer Gill instrument option 4	±3° (at 20 m/s)
Temperature	1000 Ω PRT IEC 75 1/3 class B	±0.3 °C
Humidity	HMP45C HUMICAP 180	±3% (10–90%) and ±6% (90–100%)

1.5. Scope of the present work

In summary, previous building model validation studies were mainly focused on air-conditioned buildings. Only two works were found that reported the calibration process in non-air conditioned buildings. The first one employed, as example for some steps, a closed unoccupied building without internal heat gains. For this example, results of the calibration period are shown, but none are presented for the validation period [8]. The second work carried out the entire calibration process for a naturally ventilated occupied building, but the final simulation model included a fictitious air-conditioned system to match T_i with the aim of improving the simulation prediction of ACH [16]. Among the studies that reported quantitative comparisons between simulated and measured values of T_i , range of the metrics or value (when only one work reported a metric) for the acceptance of simulation results are: for ΔT_{max} and ΔT_{min} 0.0–5.5 °C; for RMSE 0.7–2.6 °C; for m 1.0; for b 0.0–0.1 °C; for R^2 0.81 to 0.97 and for r 0.99 to 1.00.

The aim of the present work is to propose a methodology for the validation of thermal simulations of occupied and naturally ventilated non-air-conditioned buildings and to present results of the validation of a study case using eight metrics of T_i . The methodology consists of the calibration process and the validation process. The later is performed in different seasonal, occupancy and ventilation conditions. The calibration process is divided into six steps: 1) definition of the comparison variables; 2) data gathering; 3) base building model definition (divide model inputs and control variables); 4) sensitivity analysis of the control variables on T_i and on T_{si} and T_{so} (definition of control variables for first and second stages); 5) first stage of the calibration - T_i as comparison variable; and 6) second stage of the calibration - T_{si} and T_{so} as comparison variables. The study case is an office building built in Temixco, Morelos, Mexico, a hot climate region. Additionally, the building validated model is used to evaluate two strategies so as to improve thermal comfort in the building.

The paper is organized as follows. The building used as study case is described in section 2. Section 3 presents the experimental measurements. Section 4 describes the methodology of the building thermal simulations calibration. Section 5 presents the comparison between simulated and experimental results for five periods. The evaluation of the strategies to improve thermal comfort is shown in section 6. The conclusions are given in section 7.

2. Building description

The building used as study case is a five story building located in Temixco, Morelos, Mexico. It is used by postgraduate students, post-doctoral researchers and administrative staff. For this study, only the two upper levels were simulated, these two stories will be called the simulated building. The building has a rectangular base with large facades oriented to the North and South with a 6.8 °angle facing towards the Northeast and Southwest (Fig. 1(a)). Initially the simulated building was considered to be at ground level with a wind speed profile

correction to equal the wind speed at the height of the simulated building. However, the view factors with ground, air and sky for radiative heat exchange are not the same at ground level than at an 18 m height, which is the height of the base of the simulated building. The simulations here reported are made considering the simulated building at the real height and using an adiabatic condition at the simulated building floor.

The two simulated levels are occupied by offices and are connected by a central space, which has its roof at a higher level than the roof on the offices at the second level, with natural ventilation being produced by wind and thermal effects. The openings are comprised by the main door in the first level, the vents located between the roof of the second level offices and the roof of the central space, as well as all office windows and doors. The simulated building has vertical solar protections on the North and South façades, the solar protections are two stories tall, covering the height of the simulated building. The solar protections on the South façade (Figura 1(b)) are equally spaced at 60 cm from each other. On the North façade the separation of solar protections varies, being that of 60 cm on the corners of the building, increasing towards the center (Figura 1(c)).

For the validation, the Coordination Office, located on the Southwest corner of the second level is used as the control thermal zone, thus all measurements were performed in this space. The high temperature caused by the Coordination Office's orientation is the main reason why this space was selected.

3. Experimental measurements

The variables measured to create annual weather files (epw) are: direct and diffuse solar radiation, outdoor air temperature and relative humidity, atmospheric pressure, wind speed and wind direction. The outdoor variables were measured during 2018 and 2019. The indoor air temperature (T_i) was measured during different periods of October and December of 2018, as well as February, April and May of 2019. Inside surface temperature (T_{si}) and outside surface temperature (T_{so}) were measured only during the period of April 2019.

The weather data were taken from a weather station at a 10 m height from the roof of a next building, except for the diffuse solar radiation which was taken from the weather station at a 3 m height from the roof of the simulated building. Both weather stations were at a 33 m height from the ground of the studied building. The weather variables, equipment and their uncertainty are shown in Table 1.

T_i was measured in the center of the room at a 0.9 m height. T_{si} was measured for three surfaces, the roof, and the South and East walls. T_{so} was only measured for one surface, the South wall. All T_{si} and T_{so} measurement were taken from the center of the surface. The instrument used for the measurement of T_i was a heat stress monitor QUESTemp, with an uncertainty of ±0.5 °C. Thermocouples type T were used for the measurements of T_{si} and T_{so} , with an uncertainty of ±0.3 °C. Weather and temperature measurements were carried out every minute and the average values during 10 min were used to generate the epw files and to compare results.

4. Calibration of the building's thermal simulations

In this work, a methodology for the validation of thermal simulations of non-air-conditioned buildings is proposed. The validation methodology consists of a calibration process and a validation process, a flow chart is presented in Fig. 2. Simulations were performed using EnergyPlus 9.1.0.

The calibration process was divided into six steps:

Step 1) Definition of the comparison variables. The selected comparison variables are T_i , T_{si} and T_{so} .

Step 2) Data gathering. Weather and control zone temperature data were taken as described in Section 3. The geometry and dimensions of the building and the construction properties of floors, walls and roofs

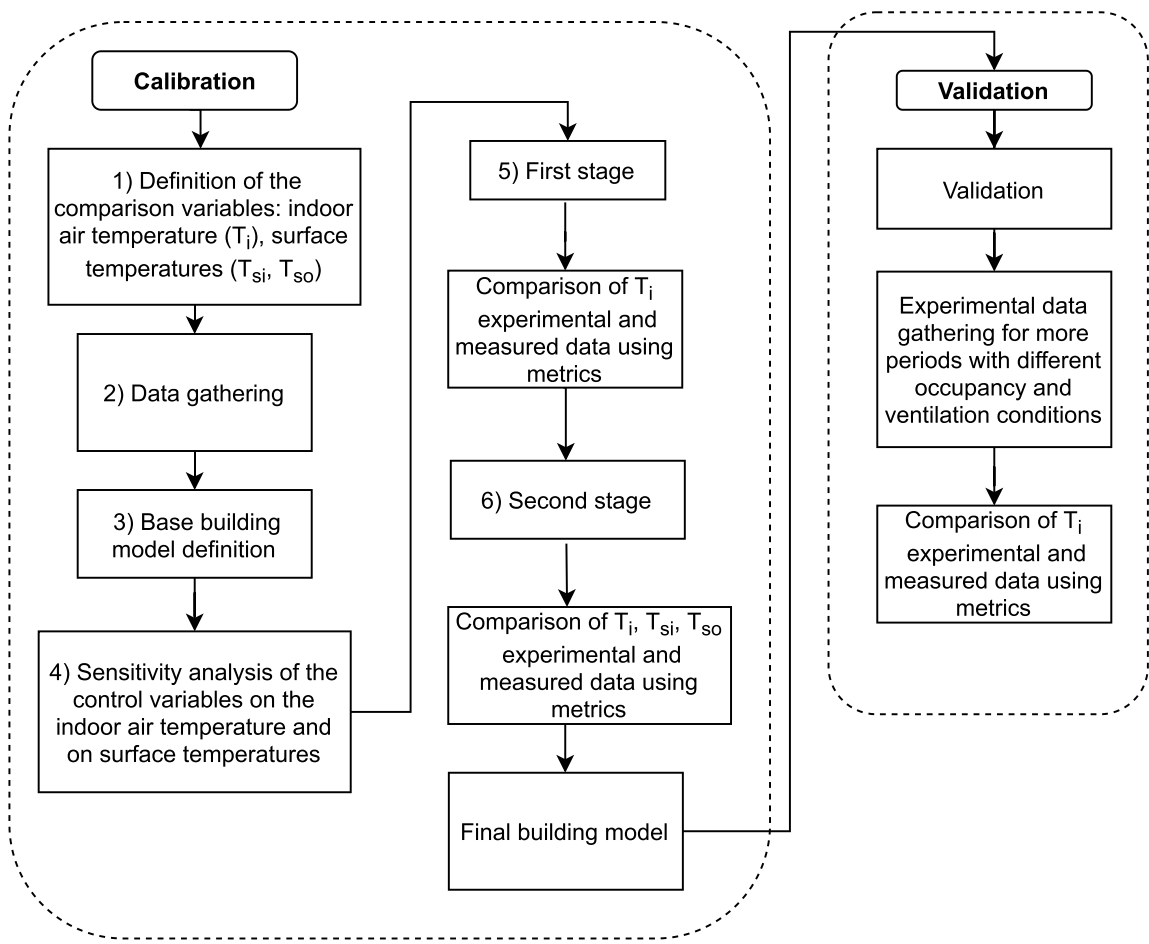


Fig. 2. Flowchart of calibration and validation processes.

Table 2

Properties of the simulated building constructions. Layers are listed from the outside to inside of the construction. Values of thickness and properties changed in the second stage of the calibration process are in parenthesis. These values are used in the final building model.

Element	Construction	Layer material	Thickness [cm]	Thermal conductivity [W/m K]	Density		Specific heat [J/kg K]	Reference
					[kg/m ³]	[kg/m ³]		
Floors Walls	Floor	High density concrete	13.0	1.35	1800	1000	[26]	
	Envelope North/South	High density concrete	8.0	1.35 (2.00)	1800 (2400)	1000	[26]	
	Envelope East/West	Hollow brick	12.0	0.70	1970	600	[26]	
	Internal type A	Aluminum	7.0	160.00	2700	1213	[27]	
	Internal type B	Hollow brick	12.0	0.70	1970	600	[26]	
	Internal type C	Gypsum	1.9	0.16	785	830	[27]	
		Air	0.3	0.02	—	—	[28]	
		Gypsum	1.9	0.16	785	830	[27]	
	First level	High density concrete	24.0	1.35	1800	1000	[26]	
	Second level	High density concrete	4.0	1.35	1800	1000	[26]	
Roofs		Tezonite	15.0 (9.0)	0.16 (0.50)	400 (720)	1000	[29,30]	
		High density concrete	8.0	1.35	1800	1000	[26]	

were taken from the building's plans. The thermal properties of each material were taken from Ener-Habitat [23] and OpenStudio [24], their values are within the range given by Ref. [25]. Table 2 shows the construction properties used for the base building model. The walls are classified both into envelope and internal walls. There were three types of internal walls: A) separates a thermal zone from the central thermal zone, B) separates the meeting room (thermal zone 19) from other thermal zones, and C) are within a given thermal zone (see Fig. 3). Occupancy and all window and door openings in the Coordination Office were registered in a logbook. A building occupants survey was made

to set the occupancy and openings schedules. An audit of the use of lamps and electric equipment was made. Likewise, an audit of the furniture and internal partitions inside each thermal zone was carried out.

Step 3) Base building model definition. According to the uncertainty of the gathered data, the input data were divided into model inputs and control variables. The control variables were the ones with larger uncertainty and were varied in the sensitivity analysis.

The considerations made for the base building model were the following: the simulated building was divided into nine thermal zones,

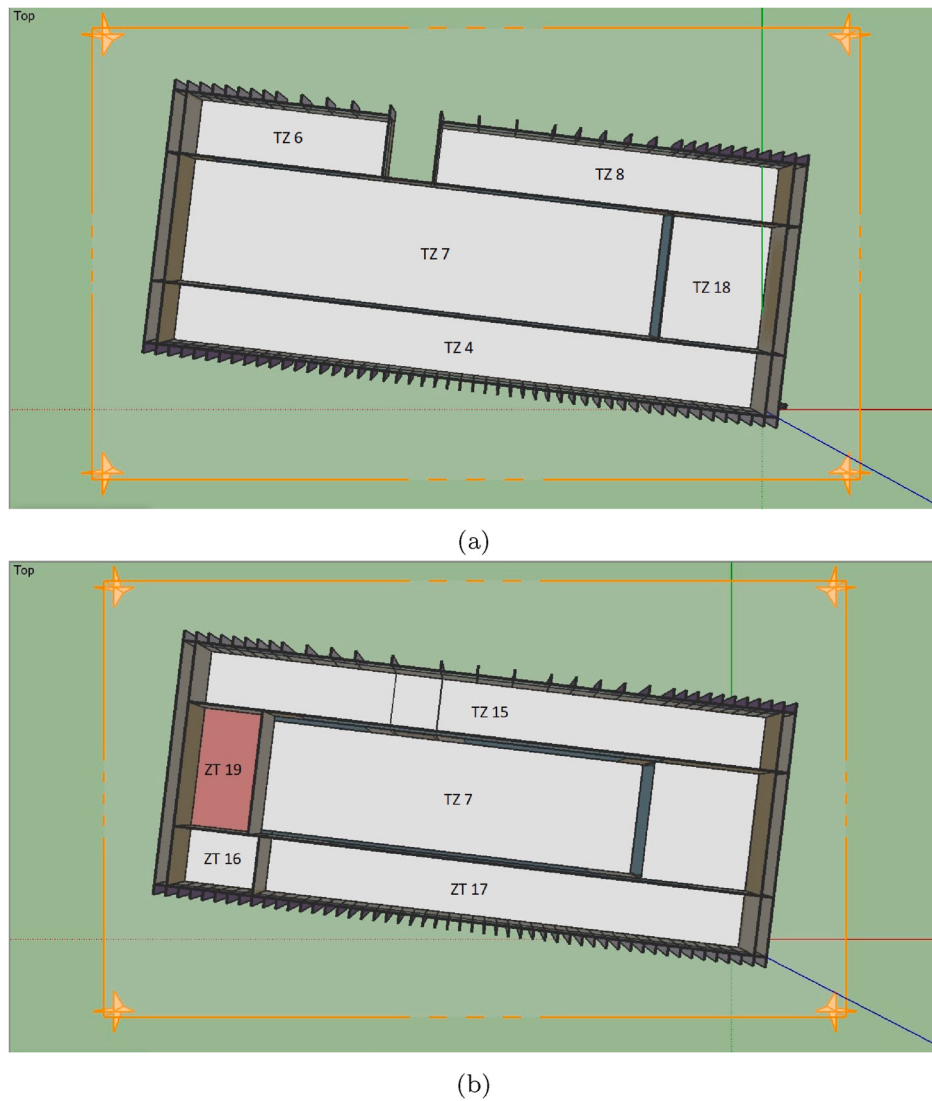


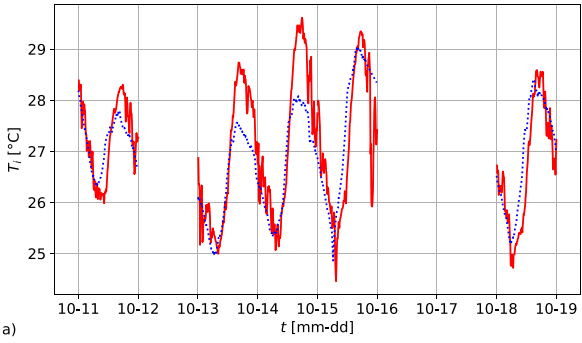
Fig. 3. Plan views from SketchUp divided by thermal zones. (a) First level and (b) second level.

shown in Fig. 3. There were four thermal zones in the first level, four thermal zones in the second level (TZ 16 corresponds to the Coordination Office) and one double height thermal zone in the center of the simulated building (TZ 7). The wind speed profile characteristics were the same for the weather station as for the building, corresponding to urban terrain. Natural ventilation and infiltration were simulated using the Airflow Network model (AFN) from EnergyPlus. Openings schedule, wind pressure coefficients and discharge coefficients were considered as model inputs. Openings schedule were taken from the survey. Wind pressure coefficients were taken from the program calculations. Because they were large openings the discharge coefficient was set at 0.6 for all openings in the detailed opening component [31,32]. Internal loads produced by lights were considered as model inputs. They were calculated taking into account the power consumption of each type of lamp and the number of lamps in each space. Internal loads by electrical equipment were also considered model inputs, and were estimated taking into account that on average, the administrative staff and professors each used a PC with a power consumption of 300 W, and that each student used a laptop with a consumption of 70 W. An extra 10% in the amount of power was added to take into account cellphones and other electrical equipment not previously taken into consideration. A fraction of the internal loads generated by both lights and electrical equipment were considered in the schedule for weekdays and weekends

according to user information. The activity level of all occupants was set to 120 W with a 0.3 radiant fraction and a 0.7 sensible fraction. The internal mass was considered a model input calculated considering the furniture and internal partitions inside each thermal zone. For the occupancy condition setting, the simulated building was divided into two: the Coordination Office and the rest of the simulated building. The Coordination Office was unoccupied and all openings were closed. The weekday schedules for occupancy and all window and door openings for natural ventilation in the rest of the simulated building were considered from 07:00 to 21:00, with different percentages of maximum office occupancy during these hours, which remained the same during the five weekdays and from month to month, according to the survey data. During weekends, the building was unoccupied and windows and doors remained closed.

The infiltration in the building was an unknown data. Although the number of occupants for the rest of the offices was known from the survey carried out for this study, there were other people who entered the building during short periods of time. This number was an unknown data, and it was considered to be a percentage of all occupants. Thus, infiltration and internal loads by people who entered the building during short periods were used as control variables.

The West and East walls were double walls, each of them constructed with hollow bricks and separated by 60 cm. The air gap was simulated as



a)

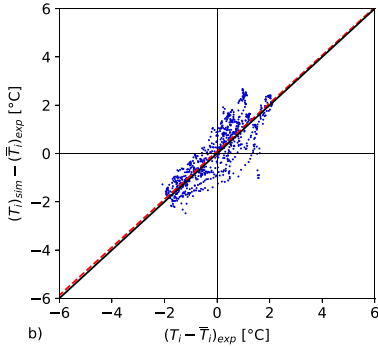
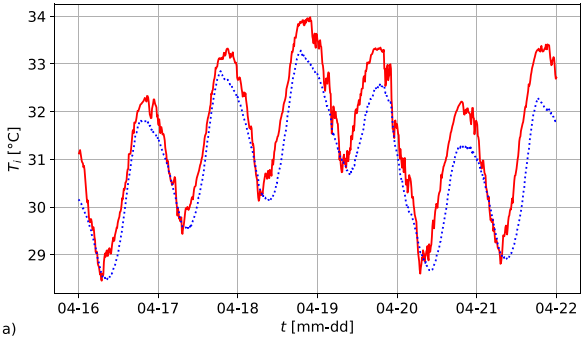


Fig. 4. Comparison between simulated and experimental results during the period of October. A) T_i as a function of time. Red and blue lines represent the simulated and experimental data, respectively, b) the simulated T_i with respect to the experimental T_i , subtracting the time average of the experimental T_i , $(\bar{T}_i)_{exp}$ from both. Red and black lines are the linear fit to the data and the ideal linear fit, respectively. (For interpretation of the references to color in this figure legend, the reader is referred to the Web version of this article.)

Table 3
Results of the T_i metrics for the period of October.

Comparison variable	ΔT_{max} [$^{\circ}C$]	ΔT_{min} [$^{\circ}C$]	ΔT_{mean} [$^{\circ}C$]	RMSE [$^{\circ}C$]	m [-]	b [$^{\circ}C$]	R^2 [-]	r [-]
T_i	0.7	-0.3	0.1	0.7	1.0	0.1	0.84	0.84



a)

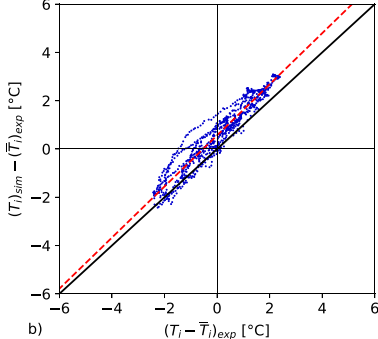


Fig. 5. Comparison between simulated and experimental results in the period of April. A) T_i as a function of time. Red and blue lines represent the simulated and experimental data, respectively, b) the simulated T_i with respect to the experimental T_i , subtracting the time average of the experimental T_i , $(\bar{T}_i)_{exp}$ from both. Red and black lines represent the linear fit to the data and the ideal linear fit, respectively. (For interpretation of the references to color in this figure legend, the reader is referred to the Web version of this article.)

a thermal zone and each brick wall was simulated with the EHLS method proposed in Ref. [14].

Among all construction properties the ones that showed the largest uncertainty were: the roughness of all walls and roofs, the thermal conductivity and density of the South and North walls, as well as the thermal conductivity, density and thickness of a layer on the second level roof. This layer was used as lightweight aggregate with variable thickness to form a slope for rain drainage. In the simulations the thickness of this layer, made of tezontle, was considered the same for the entire building. All former variables were considered as control variables. The properties of the materials were varied within the ranges given by Ref. [25], and the thickness of the tezontle layer was varied within the range given in the architectural plans.

Step 4) Sensitivity analysis. A sensitivity analysis of the control variables on T_i and on T_{si} and T_{so} was undertaken to define the control variables for the first and second stages. The sensitivity analysis was made by varying the control variables within their uncertainty range, during a given time period in October. The results showed that the infiltration and the internal loads by people who entered the building during short periods were the variables with the most impact on T_i , while the construction properties mainly affected T_{si} and T_{so} .

Step 5) First stage of calibration. In this stage, T_i was used as a comparison variable and the infiltration and internal loads by people were used as control variables. The infiltration mainly impacted the amplitude of T_i , while the internal loads by people mainly affected the average of T_i . The values of infiltration and internal loads by people who entered the building during short periods that reduce the metrics of T_i were used as model inputs in the second stage.

Step 6) Second stage of calibration. In this stage, T_{si} , T_{so} , as well as T_i , were used as comparison variables. The control variables for this stage were the roughness, thermal conductivity and density of the South and North walls to match T_{si} and T_{so} for the South wall; the roughness of the West wall to match this wall T_{si} ; the roughness of the outside layer and the thermal conductivity, density and thickness of the roof tezontle layer to match T_{si} of the roof. The values for these construction properties that enhanced the metrics for the comparison variables were used for the final building model employed in the validation process.

Eight metrics were used for the comparison between simulations and experimental results in the two calibration stages and the validation process: the average of the difference between simulated and experimental daily maximum temperature (ΔT_{max}); the average of the difference between simulated and experimental daily minimum temperature (ΔT_{min}); the average of the difference between simulated and experimental daily mean temperature (ΔT_{mean}); the root mean square error (RMSE) that provides the average of the absolute value of the difference between simulated and experimental temperature at each time-step; the slope (m), the intercept (b) and the correlation coefficient (R^2) of the linear fit of the simulated temperature as a function of the experimental temperature, both temperatures minus the experimental mean value; and the Pearson's index (r) that provides a direct correlation between simulated and experimental results [8].

4.1. First stage results

The period in October was the first to be measured during this work, and was used for the first stage simulations. During this period, the

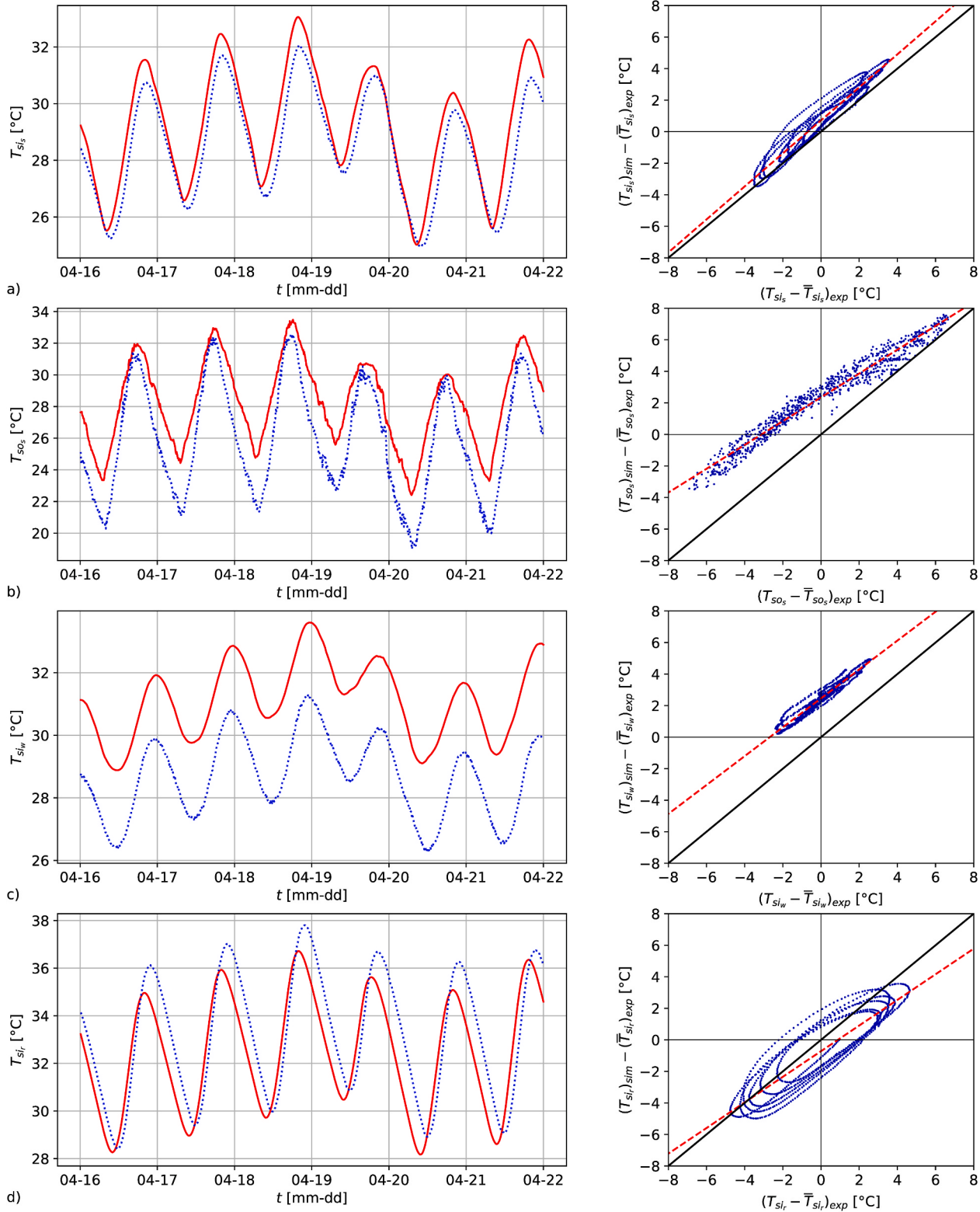


Fig. 6. Comparison between simulated and experimental results. Left side T_{si} and T_{so} as a function of time. Red and blue lines represent the simulated and experimental data, respectively. Right side the simulated T_{si} and T_{so} with respect to the experimental T_{si} and T_{so} , for all temperatures, the values are given subtracting the time average of the experimental value.

Red and black lines are the linear fit to the data and the ideal linear fit, respectively. For a) T_{si_s} , b) T_{so_s} , c) T_{si_w} , d) T_{si_r} . (For interpretation of the references to color in this figure legend, the reader is referred to the Web version of this article.)

Table 4

Temperature metrics results for the period in April.

Journal of Building Engineering 44 (2021) 102922

Comparison variable	ΔT_{max} [°C]	ΔT_{min} [°C]	ΔT_{mean} [°C]	RMSE [°C]	m [-]	b [°C]	$R2$ [-]	r [-]
T_{sis}	0.8	0.2	0.7	0.9	1.0	0.7	0.96	0.96
T_{sos}	0.0	1.4	1.1	0.9	0.8	2.4	0.98	0.98
T_{siw}	2.4	2.7	2.5	2.5	0.9	2.5	0.97	0.97
T_{sir}	-1.1	-0.4	-0.7	1.5	0.8	-0.7	0.87	0.87
T_i	0.7	0.0	0.6	0.7	1.1	0.6	0.96	0.96

Table 5Metrics for T_i for the five periods. The season and occupancy conditions are included. The occupancy condition is shown as occupied (O) and unoccupied (NO), in the Coordination Office - in the rest of the simulated building.

Period	Season	Occupancy	ΔT_{max} [°C]	ΔT_{min} [°C]	ΔT_{mean} [°C]	RMSE [°C]	m [-]	b [°C]	$R2$ [-]	r [-]
October	Transition	NO-O	0.3	0.0	0.0	0.6	0.9	0.0	0.86	0.86
December	Semi-cold	NO-NO	0.3	0.0	0.2	0.6	1.1	0.2	0.95	0.95
February	Transition	NO-O	0.3	0.2	0.3	0.6	0.9	0.3	0.94	0.94
April	Hot	NO-NO	0.7	0.0	0.6	0.7	1.1	0.0	0.96	0.96
May	Hot	O-O	0.4	-0.3	0.3	0.5	1.1	0.0	0.98	0.98

Coordination Office was unoccupied, its windows and door were remained closed. The rest of the simulated building was occupied during work hours of weekdays, its windows and doors were opened during occupancy, and remained closed when it was unoccupied.

In AFN, the infiltration was controlled by the air mass flow coefficient, so that this coefficient was varied to match T_i amplitude with experimental results. Best results were obtained with a value of 0.02, which produced an average of $ACH = 0.4 \text{ l/h}$. The number of people who entered the building for short periods was considered proportional to the number of occupants for each hour given by the schedule. The number of people who entered the building for short periods that minimize the difference between simulated and measured averages of T_i was 25% of the building's occupants.

Fig. 4 presents the qualitative comparison between simulated and experimental results of T_i as a function of time, as well as the simulated T_i with respect to the experimental T_i . Table 3 presents the results of the metrics for T_i for the period in October. From these results, it can be seen that the maximum difference between simulated and experimental T_i is 0.7°C for both ΔT_{max} and RMSE; and that the values of $R2$ and r are over 0.75, which is the minimum acceptable value according to Ref. [11].

4.2. Second stage results

The period in April was used for the second stage of calibration. The months of April and May are the hottest months of the year in Temixco, Morelos, Mexico, and thus represent the critical hot condition for the building. The period in April was selected for the second stage since for this period the simulated building was unoccupied and remained closed, this means that only-infiltration was considered. This condition increased the impact of heat transfer through the envelope mainly affecting surface temperatures that were used as comparison variables in this second stage. The change in the roughness of all outside layer materials belonging to the constructions, from 'smooth' (the default in EnergyPlus and used in the first stage) to 'rough', improved all metrics for all temperatures, specially for T_{sos} and T_{siw} , the sub-indexes s and w specify the South and West walls, respectively. Changing the materials' properties generally improved the metrics. The largest improvement was obtained for ΔT_{mean} which changed from 4.5°C to 2.5°C . The changes in the properties' values from the base building model to the final building model can be seen in Table 2. Note that the increase in thermal conductivity for the high density concrete and that of the tezontle were accompanied by an increase to their respective densities, which is the expected relationship between these properties in this type of materials.

Figs. 5 and 6 present the qualitative comparison between simulated and experimental results of temperature as a function of time and the simulated temperature with respect to the experimental temperature for T_i , T_{sis} , T_{sos} , T_{siw} and T_{sir} (sub-index r is for roof), respectively. The simulated results reported here were obtained once the changes to the roughness and material properties were made. The metric results are presented in Table 4, in it, it can be seen that for all temperatures, $R2$ is over 0.75. The temperature with the largest value of ΔT_{mean} is T_{siw} . This can be due to the difficulty in simulating the double wall on the West façade which also receives the highest amount of solar radiation. It seems that the overestimation in T_{siw} is compensated with the underestimation of T_{sir} in the effect that both exerted on T_i , which also has an overestimation, yet lower than that of T_{siw} . It can be noted that during the period in April, $R2$ and r for T_i were larger than those obtained in the first stage for the period in October (Table 3).

5. Validation

For the validation process five time periods with different seasonal, occupancy and ventilation conditions were tested. The seasonal, as well as the occupancy condition for the Coordination Office and for the rest of the simulated building are specified for each period in Table 5. When the space was occupied there was natural ventilation, while when it was unoccupied there was only infiltration.

Qualitative comparisons between simulated and experimental results of T_i as a function of time and the simulated T_i with respect to the experimental T_i , for the periods in October, December, February and May are shown in Fig. 7. The simulated T_i in October had better results than that obtained in the first stage (4), the difference between simulated and experimental temperature amplitude was reduced. In December, the simulated T_i had a similar behavior to that of the experimental, with a small difference in temperature amplitude. In February, the behavior of simulated T_i was similar to the experimental one, showing a small delay and an overestimation lower than 1°C . The simulated T_i in May, showed the best qualitative agreement with experimental T_i .

Table 5 shows the results of the metrics for T_i during all periods. It can be observed that for all periods all metrics with temperature units have positive values (except ΔT_{min} in May), indicating an overestimation less or equal to 0.7°C . In all periods, m is equal to 1.0 ± 0.1 , and in most, b is 0.0°C reaching a maximum of 0.3°C . $R2$ and r are over 0.85, which indicates a good correlation between experimental and simulated T_i . The metrics for the period in October improved with respect to the corresponding values from the first stage simulations (3), indicating the convenience in carrying out the second stage. The period

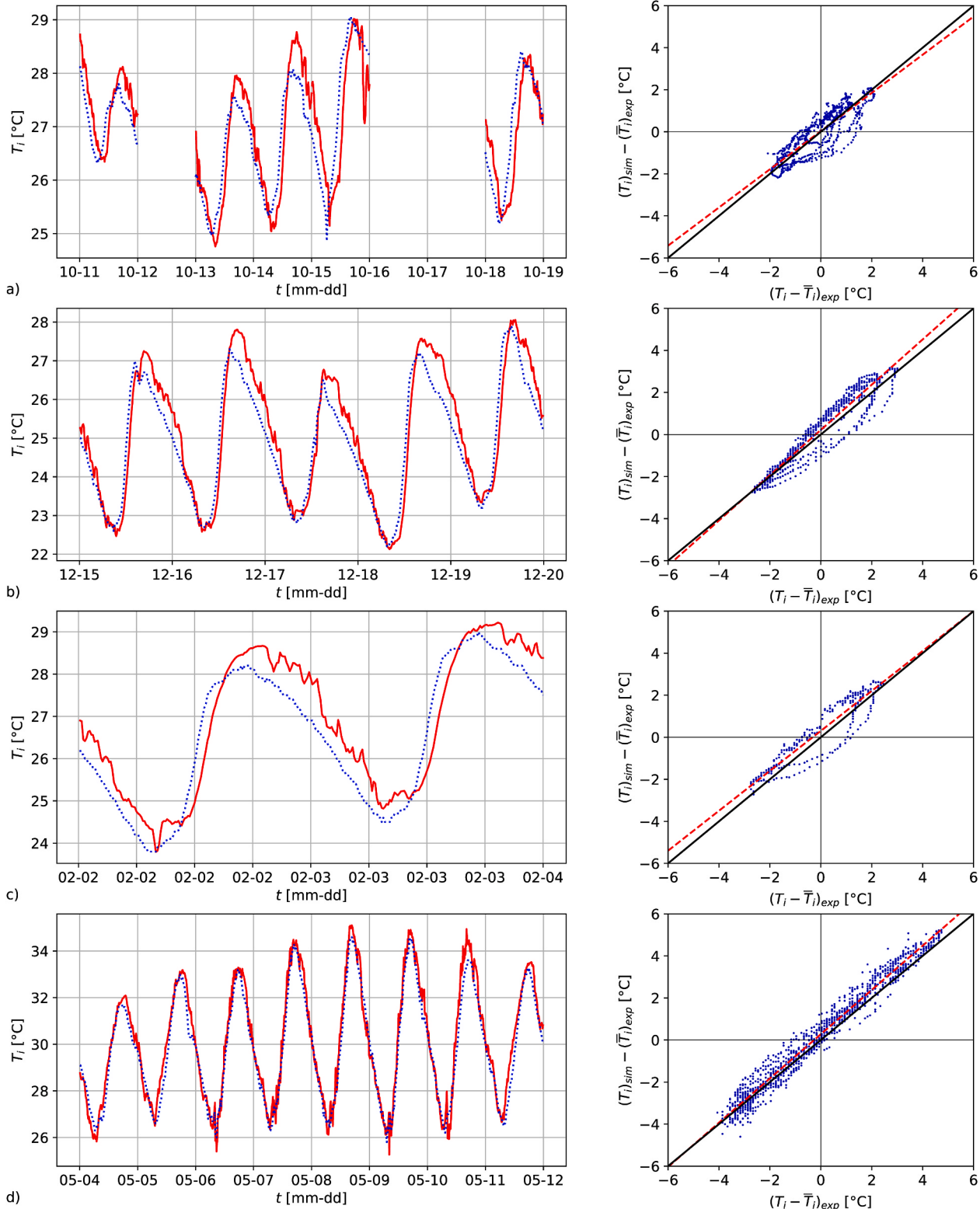


Fig. 7. Comparison between simulated and experimental results. Left side T_i as a function of time. Red and blue lines represent the simulated and experimental data, respectively. Right side the simulated T_i with respect to the experimental T_i , for all temperatures, the values are given subtracting the time average of the experimental value.

Red and black lines are the linear fit to the data and the ideal linear fit, respectively. For the periods in a) October, b) December, c) February, d) May. (For interpretation of the references to color in this figure legend, the reader is referred to the Web version of this article.)

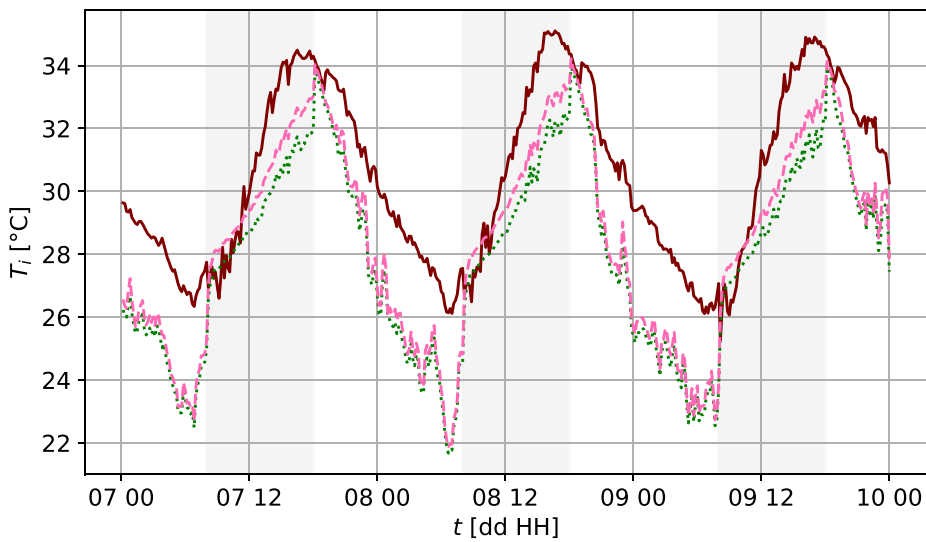


Fig. 8. Impact of strategies on the Coordination Office T_i for three days during May. Base case (B) - dark brown solid line, night ventilation case (NV) - dashed pink line, and night ventilation with white colored outside building envelope (NV-W) - dotted green line. Vertical gray areas represent occupancy hours in the Coordination Office. (For interpretation of the references to color in this figure legend, the reader is referred to the Web version of this article.)

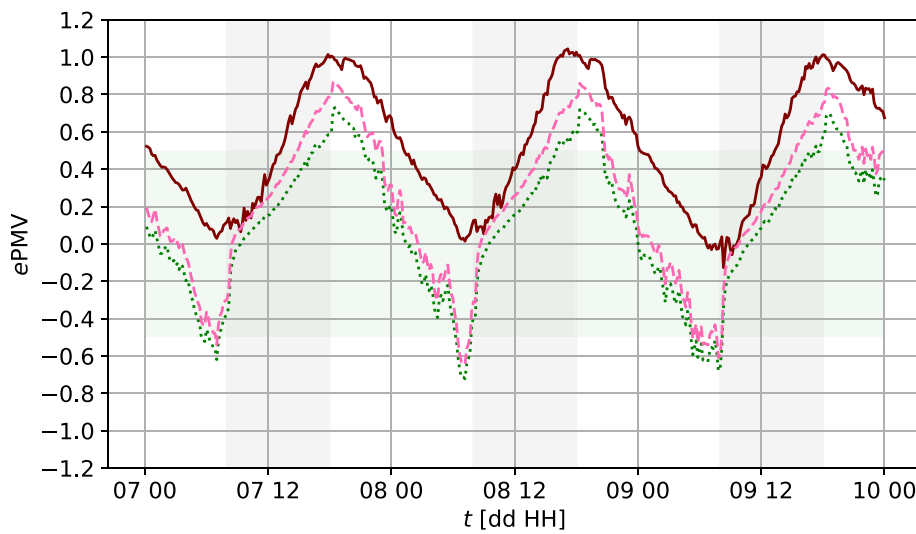


Fig. 9. Impact of strategies on the ePMV of the Coordination Office for three days in May. Base case (B) - dark brown solid line, night ventilation case (NV) - dashed pink line and night ventilation with white colored outside building envelope (NV-W) - dotted green line. The vertical gray areas represent the occupancy hours in the Coordination Office and the green horizontal area represents the comfort zone. (For interpretation of the references to color in this figure legend, the reader is referred to the Web version of this article.)

in May showed the best RMSE, R2 and r results.

The values of ΔT_{max} and ΔT_{min} are smaller than the maximum accepted value reported in the literature, 5.5 °C. Also, the values of RMSE are smaller than the maximum reported in the literature, 2.6 °C. The values of R2 are larger than the minimum accepted value in the literature, 0.81.

6. Strategies to improve thermal comfort

In this section two strategies to improve the thermal comfort of the building are tested by performing simulations using the validated final building model. The first strategy is the use of night ventilation (NV). NV implies that when the Coordination Office and the rest of the building are unoccupied, they remain closed (only with infiltration), and that when they are unoccupied, windows remain open and doors be closed. The second strategy is that of changing to the color white (W) all exterior surfaces of the building envelope.

Fig. 8 shows a qualitative comparison of T_i in the Coordination Office

between the base case (B), NV case and NV-W case, during three days of May. The B case corresponds to the building as it is actually colored and used, i.e. with natural ventilation when it is occupied, and infiltration when it is unoccupied. It can be seen that the NV case reduces the maximum T_i , in approximately 2°C, and the NV-W case in more than 3°C, when both are compared to the B case. During the initial hours of occupation, the NV and NV-W cases have slightly higher values of T_i than the B case because at that time the outdoor air temperature is lower than T_i and can reduce the T_i value when windows are opened, as in the B case. The case W is not shown in the figure because its impact on T_i is not significant.

To evaluate the impact of the strategies proposed for the building an evaluation of the thermal comfort was made. The thermal comfort was evaluated employing the extended Predicted Mean Value (ePMV) proposed in Ref. [33], which is specifically designed for non-air-conditioned buildings in hot climates. Here, $e = 0.5$ is used. The comfort range of ePMV is considered as in the standard ASHRAE-55, i.e. [-0.5, +0.5] [34]. Fig. 9 shows the ePMV for the same three days during

May showed in Fig. 8. It can be observed that the NV-W case reduces the value of ePMV as well as the amount of discomfort hours.

For a quantitative comparison the period between the 1st and 17th of May is used. This period was selected because the vacation period was still into effect before the 1st of May, and the rainy season starts after the 17th of May, ending the critical hot season. The maximum values for the ePMV are 1.1 for the B case, 0.9 for the NV case and 0.7 for the NV-W case. The percentage of discomfort hours during occupancy time are 44.8% for the B case, 32.8% for the NV case and 16.9% for the NV-W case. These results show that a significant reduction in discomfort during occupancy hours can be achieved by a change in ventilation habits, from day ventilation to night ventilation, as well as a change to white color for the outside surface of the building envelope.

7. Conclusions

In this work a methodology for the validation of thermal simulations of non-air-conditioned buildings is proposed. It consists of a calibration process and a validation process.

The main differences in this methodology which contrast from the two previously reported for non-air-conditioned buildings are: i) the separation of data inputs which values are known with uncertainties into those that have more influence on the indoor air temperature of the control zone from those with more impact on the surface temperatures of the control zone; ii) to carry out the calibration process into two stages, the first one using as the comparison variable the indoor air temperature, and the second one adding as comparison variables the surface temperatures; and iii) to carry out the validation process in different seasonal, occupancy and ventilation conditions. Identifying which control variables have more influence over the indoor air temperature and which exert more influence over surface temperatures allows for the calibration to be divided into two stages: one to match the indoor air temperature and one to match the surface temperatures of each wall and roof varying only their corresponding properties. This significantly reduces the number of simulations that have to be done in order to find the values for the control variables that minimize the metrics for the comparison variables. As it was done in the present work for the study case, it is recommended that the second stage is made during the hottest season when the high solar radiation and outdoor temperature produce the highest possible effect of the construction properties on surface temperatures.

Results show that the metrics of the indoor air temperature improve values in the second stage when compared to those obtained in the first stage. And that inside surface temperatures change up to 2°C , which impacts on thermal comfort predictions.

The validation results show that the building model obtained from the calibration process is suitable to simulate the building in different seasonal, occupancy and ventilation conditions, and can likewise be used with confidence to test strategies used to improve thermal comfort for the building.

Two simple strategies to improve thermal comfort in the case study building were tested: a change in ventilation habits consisting of switching from ventilation during occupancy to night ventilation and the change to white for the building facade color. When these two strategies are combined the percentage of discomfort hours during occupancy time is significantly reduced with respect to the actual building conditions from 44.8% to 16.9%.

CRediT authorship contribution statement

I. Calixto-Aguirre: Methodology, Software, Data curation, Visualization, Investigation, Writing – original draft. **G. Huelsz:** Conceptualization, Methodology, Investigation, Writing – review & editing. **G. Barrios:** Software, Supervision, Writing – review & editing. **M.V. Cruz-Salas:** Software, Supervision, Writing – review & editing.

Declaration of competing interest

Journal of Building Engineering 44 (2021) 102922

The authors declare that they have no known competing financial interests or personal relationships that could have appeared to influence the work reported in this paper.

Acknowledgments

The authors would like to thank Jesús Quiñones for providing the weather data. This work is part of the S0019-2017-01-291600 project, sponsored by the CONACYT - SENER- Energy Sustainability Fund.

References

- [1] International Energy Agency (IEA), International energy agency and international partnership for energy efficiency cooperation: building energy performance metrics, *Building Science Digest* 4 (8). doi:10.1016/j.jobc.2017.06.011.
- [2] A. Fouquier, S. Robert, F. Suard, L. Stéphan, A. Jay, State of the art in building modelling and energy performances prediction: a review, *Renew. Sustain. Energy Rev.* 23 (2013) 272–288, <https://doi.org/10.1016/j.rser.2013.03.004>.
- [3] V. Harish, A. Kumar, A review on modeling and simulation of building energy systems, *Renew. Sustain. Energy Rev.* 56 (2016) 1272–1292, <https://doi.org/10.1016/j.rser.2015.12.040>.
- [4] Y. Lu, J. Dong, J. Liu, Zonal modelling for thermal and energy performance of large space buildings: a review, *Renew. Sustain. Energy Rev.* 133. doi:10.1016/j.rser.2020.110241.
- [5] U.S. Department of Energy (DOE), *EnergyPlus V. 9.1 Documentation. Engineering Reference*, U.S. Department of Energy, 2016.
- [6] T. Reddy, Literature review on calibration of building energy simulation programs: Uses, problems, procedure, uncertainty, and tools 112 (PART 1) (2005) 226–240.
- [7] P. Raftery, M. Keane, J. O'Donnell, Calibrating whole building energy models: an evidence-based methodology, *Energy Build.* 43 (9) (2011) 2356–2364, <https://doi.org/10.1016/j.enbuild.2011.05.020>.
- [8] R. Pernetti, A. Prada, P. Baggio, The calibration process of building energy models, in: *Green Energy and Technology Building Refurbishment for Energy Performance A Global Approach*, Springer International Publishing Switzerland, 2014.
- [9] Y. Sang, J.R. Zhao, J. Sun, B. Chen, S. Liu, Experimental investigation and EnergyPlus-based model prediction of thermal behavior of building containing phase change material, *Journal of Building Engineering* 12 (June) (2017) 259–266, <https://doi.org/10.1016/j.jobc.2017.06.011>.
- [10] K.W.C. Dahanayake, C.L. Chow, Studying the potential of energy saving through vertical greenery systems: using EnergyPlus simulation program, *Energy Build.* (2017) 47–59, <https://doi.org/10.1016/j.enbuild.2016.12.002>.
- [11] A.S. Andelković, I. Mujan, S. Dakić, Experimental validation of a EnergyPlus model: application of a multi-storey naturally ventilated double skin façade, *Energy Build.* (2016) 27–36, <https://doi.org/10.1016/j.enbuild.2016.02.045>.
- [12] E. Simá, M.A. Chagolla-Aranda, G. Huelsz, R. Tovar, G. Alvarez, Tree and neighboring buildings shading effects on the thermal performance of a house in a warm sub-humid climate, *Building Simulation* (2015) 1–13, <https://doi.org/10.1007/s12273-015-0247-2>.
- [13] J. Yang, H. Fu, M. Qin, Evaluation of different thermal models in EnergyPlus for calculating moisture effects on building energy consumption in different climate conditions, in: *Procedia Engineering*, 2015, pp. 1635–1641, <https://doi.org/10.1016/j.proeng.2015.09.194>.
- [14] G. Barrios, J. Rojas, G. Huelsz, R. Tovar, S. Jalife-Lozano, Implementation of the equivalent-homogeneous-layers-set method in whole-building simulations: experimental validation, *J. Build. Phys.* 35 (2017), <https://doi.org/10.1177/1744259115559193>.
- [15] A. Barbaresi, F. De Maria, D. Torreggiani, S. Benni, P. Tassinari, Performance assessment of thermal simulation approaches of wine storage buildings based on experimental calibration, *Energy Build.* 103 (2015) 307–316, <https://doi.org/10.1016/j.enbuild.2015.06.029>.
- [16] A. Belleri, R. Lollini, S. Dutton, Natural ventilation design: an analysis of predicted and measured performance, *Build. Environ.* 81 (2014) 123–138, <https://doi.org/10.1016/j.buildenv.2014.06.009>.
- [17] P. Raftery, M. Keane, A. Costa, Calibrating whole building energy models: detailed case study using hourly measured data, *Energy Build.* 43 (12) (2011) 3666–3679, <https://doi.org/10.1016/j.enbuild.2011.09.039>.
- [18] D. Coakley, P. Raftery, P. Molloy, Calibration of whole building energy simulation models: detailed case study of a naturally ventilated building using hourly measured data, *Proceedings First Building Simulation and Optimization Conference* (2012) 57–64.
- [19] P. Hayes, P. Linden, G. da Graça, Use of simulation in the design of a large, naturally ventilated office building, *Build. Serv. Eng. Technol.* 25 (3) (2004) 211–221, <https://doi.org/10.1191/0143624404bt102oa>.
- [20] A. Roetzel, A. Tsangrassoulis, Impact of climate change on comfort and energy performance in offices, *Build. Environ.* 57 (2012) 349–361, <https://doi.org/10.1016/j.buildenv.2012.06.002>.
- [21] N. Martins, G. Carrilho da Graça, Impact of outdoor PM2.5 on natural ventilation usability in California's nondomestic buildings, *Appl. Energy* 189 (2017) 711–724, <https://doi.org/10.1016/j.apenergy.2016.12.103>.

- [22] J. Liu, Y. Liu, L. Yang, T. Liu, C. Zhang, H. Dong, Climatic and seasonal suitability of phase change materials coupled with night ventilation for office buildings in western China, *Renew. Energy* 147 (2020) 356–373, <https://doi.org/10.1016/j.renene.2019.08.069>.
- [23] G. Huelsz, G. Barrios, J. Rojas, Ener-habitat: evaluación térmica de la envolvente arquitectónica. manual de uso, <http://www.enerhabitat.unam.mx>, 2013.
- [24] National Renewable Energy Laboratory and Argonne National Lab and Lawrence Berkeley National Lab and Oak Ridge National Lab and Pacific Northwest National Lab, OpenStudio, 2020.
- [25] American Society of Heating and Air-Conditioning Engineers, ASHRAE Standard 26-2009: Heat, Air, and Moisture Control in Building Assemblies, ASHRAE Standard 26-2009, 2009, 25.1–25.16.
- [26] Ier-Unam, Unison, Uat, Cenidet, Uam, Ener-Habitat, URL, <http://www.enerhabitat.unam.mx>.
- [27] Nrel, Anl, Lbnl, Ornl, Pnn, Openstudio, URL, <https://www.openstudio.net/downloads>, 2013.
- [28] Y.A. Cengel, M.A. Boles, *Thermodynamics: an Engineering Approach*, McGraw Hill, 2018.
- [29] A. Cedeño, Materiales bioclimáticos, Teconología, medioambiente y sostenibilidad (*Journal of Building Engineering* 44 (2021) 102922) 100–110Asociación de Empresas para el Ahorro de Energía en la Edificación, North America Insulation Manufacturers Association and Environment Canada.
- [30] O. Cortés, Análisis térmico de los sistemas constructivos comunes utilizados en techos y muros en vivienda versus la normatividad oficial en el tema, en los diversos bioclimas de México, universidad Nacional Autónoma de México (UNAM), 2008.
- [31] N.B. Kaye, G.R. Hunt, Time-dependent flows in an emptying filling box, *J. Fluid Mech.* 520 (2004) 135–156, <https://doi.org/10.1017/S0022112004001156>.
- [32] J.L. Partridge, P.F. Linden, Validity of thermally-driven small-scale ventilated filling box models, *Exp. Fluid* 54 (11) (2013) 1613, <https://doi.org/10.1007/s00348-013-1613-4>.
- [33] P. Fanger, J. Toftum, Extension of the PMV model to non-air-conditioned buildings in warm climates, *Energy Build.* 34 (6) (2002) 533–536, [https://doi.org/10.1016/S0378-7788\(02\)00003-8](https://doi.org/10.1016/S0378-7788(02)00003-8).
- [34] American society of heating and air-conditioning engineers, ASHRAE standard 55-2017: thermal environmental conditions for human occupancy, ASHRAE Standard (2017) 66, 55-2017.